

# Nanoparticle-mediated Reactive Oxygen Species Generation in High-Intensity Focused Ultrasound

Jeffrey S. Souris<sup>1</sup>, Gregory J. Anthony<sup>1</sup>, Viktor Bollen<sup>1</sup>, Rene Maldonado<sup>1</sup>, Leu-Wei Lo<sup>1,2</sup>, Chin-Tu Chen<sup>1</sup>, and Kenneth B. Bader<sup>1</sup>  
<sup>1</sup>The University of Chicago, Chicago, IL, USA; <sup>2</sup>National Health Research Institutes, Zhunan, Miaoli, Taiwan

## Introduction

High-intensity focused ultrasound (HIFU) is an emerging therapeutic modality that employs ultrasonic pressure wave-packets to induce highly localized destruction of pathologic tissues, primarily by direct thermal ablation and necrosis. At sufficiently high acoustic intensities, inertial cavitation is induced whereby microbubbles violently form and collapse, leading to the creation of localized shock waves that fractionate tissues mechanically via shear forces (aka histotripsy). While such non-thermal ablation is more clinically desirable, due to the human body's ability to better eliminate the fragmented/liquefied cellular aftermath, it is intrinsically a somewhat stochastic process and thus difficult to monitor and control. To this end we have begun synthesizing and characterizing biocompatible nanomaterials that can serve not only as cavitation induction sites that lower the energy threshold and temperature at which cavitation onset occurs, but that also optimize the production of sonoluminescence-derived photo/sono-excitation of electron-hole pairs on the nanomaterial's surface, which then can react with local H<sub>2</sub>O and adsorbed gas molecules to produce highly cytotoxic reactive oxygen species (ROS).

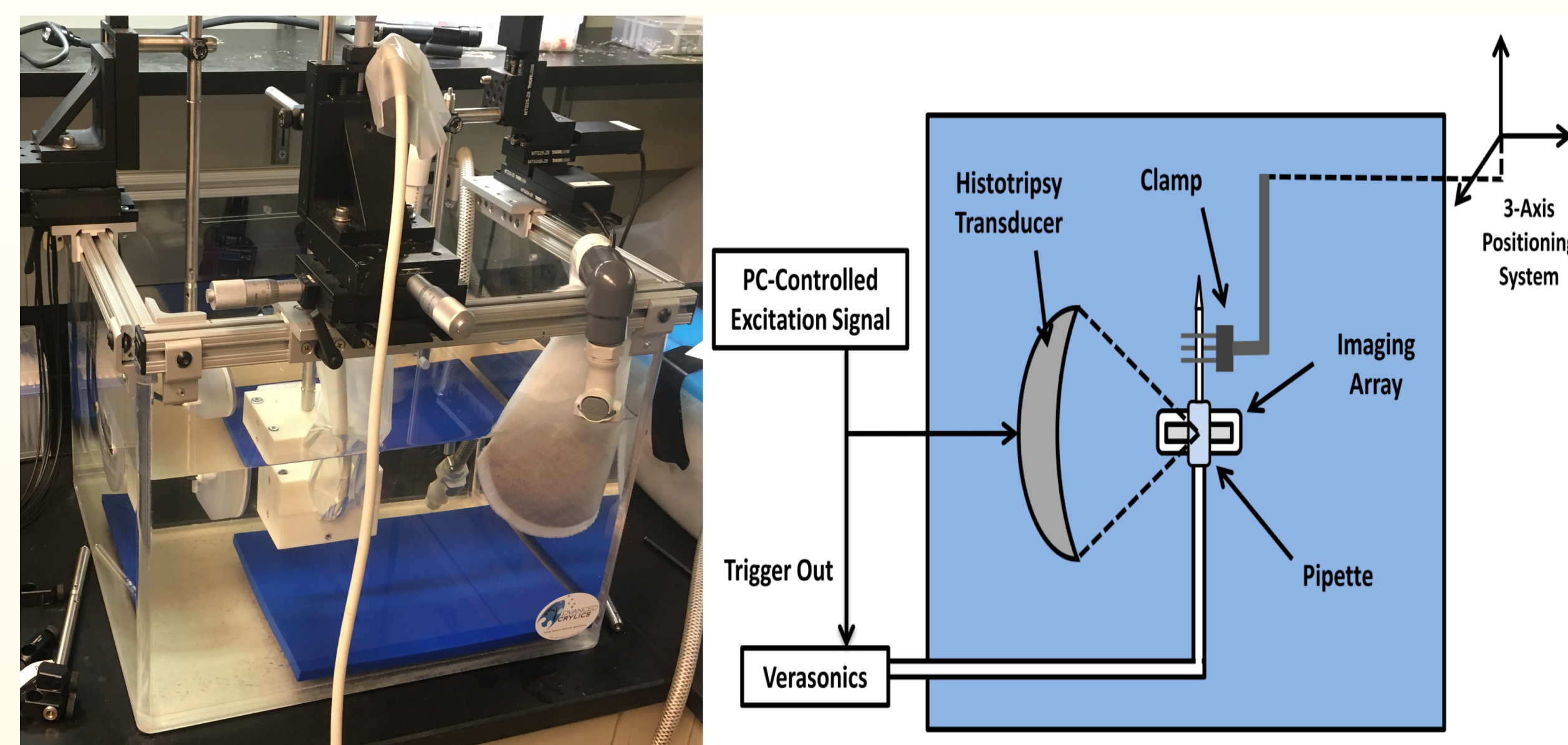
## Methods and Materials

In the current study we examined 4 nanomaterials of roughly similar particle morphology (i.e., comparable diameter, shape, porosity, surface area) but significantly different dielectric and piezoelectric properties: 3 semiconductors (rutile TiO<sub>2</sub>, BaTiO<sub>3</sub>, and ZnO) and a wide-gap insulator (Y<sub>2</sub>O<sub>3</sub>). Nanoparticles were placed within an inverted thin-walled polyethylene transfer tube and suspended in 1 ml of 2 mM terephthalic acid – a hydroxyl radical trap – for ROS quantitation, at particle number densities selected to achieve comparable total particle surface area exposure, since ROS generation depends on both the particle's electronic structure and the particle's topology that can access ambient water.

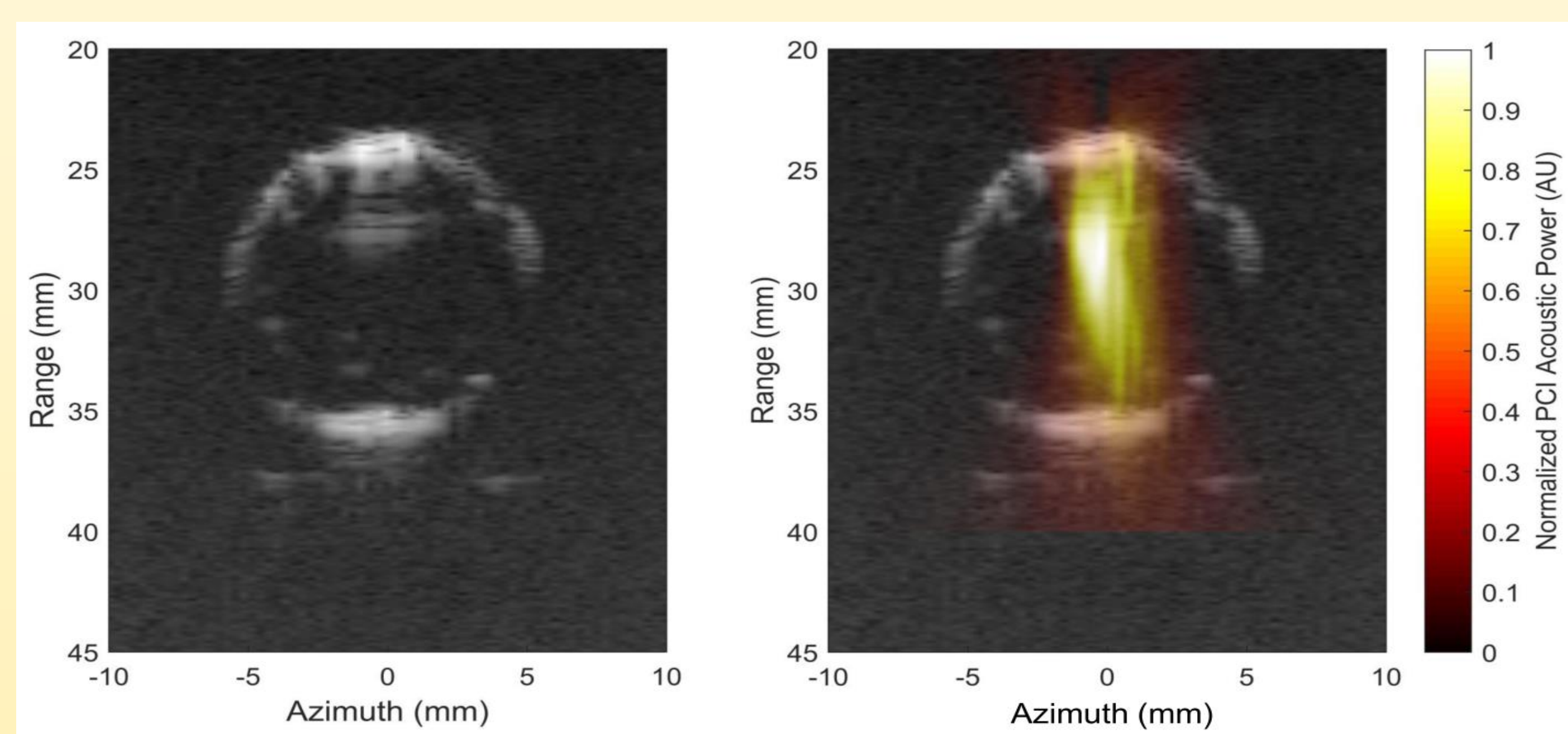
Material	Particle Diameter	Surface Area
Y <sub>2</sub> O <sub>3</sub>	37 nm	50 m <sup>2</sup> /gm
r-TiO <sub>2</sub>	32 nm	45 m <sup>2</sup> /gm
BaTiO <sub>3</sub>	58 nm	20 m <sup>2</sup> /gm
ZnO	25 nm	50 m <sup>2</sup> /gm

A calibrated 10.0 cm diameter, spherically-shaped, 8-segment ultrasound transducer of 7.5 cm focal length and 1 MHz center-frequency, served as the HIFU source, while a 4.0 cm long, linear-array ultrasound transducer

was positioned orthogonal to the direction of sound wave propagation near the transfer tube, to monitor the induced cavitation within the specimen during insonation. With the HIFU source stationary, both the linear-array imaging

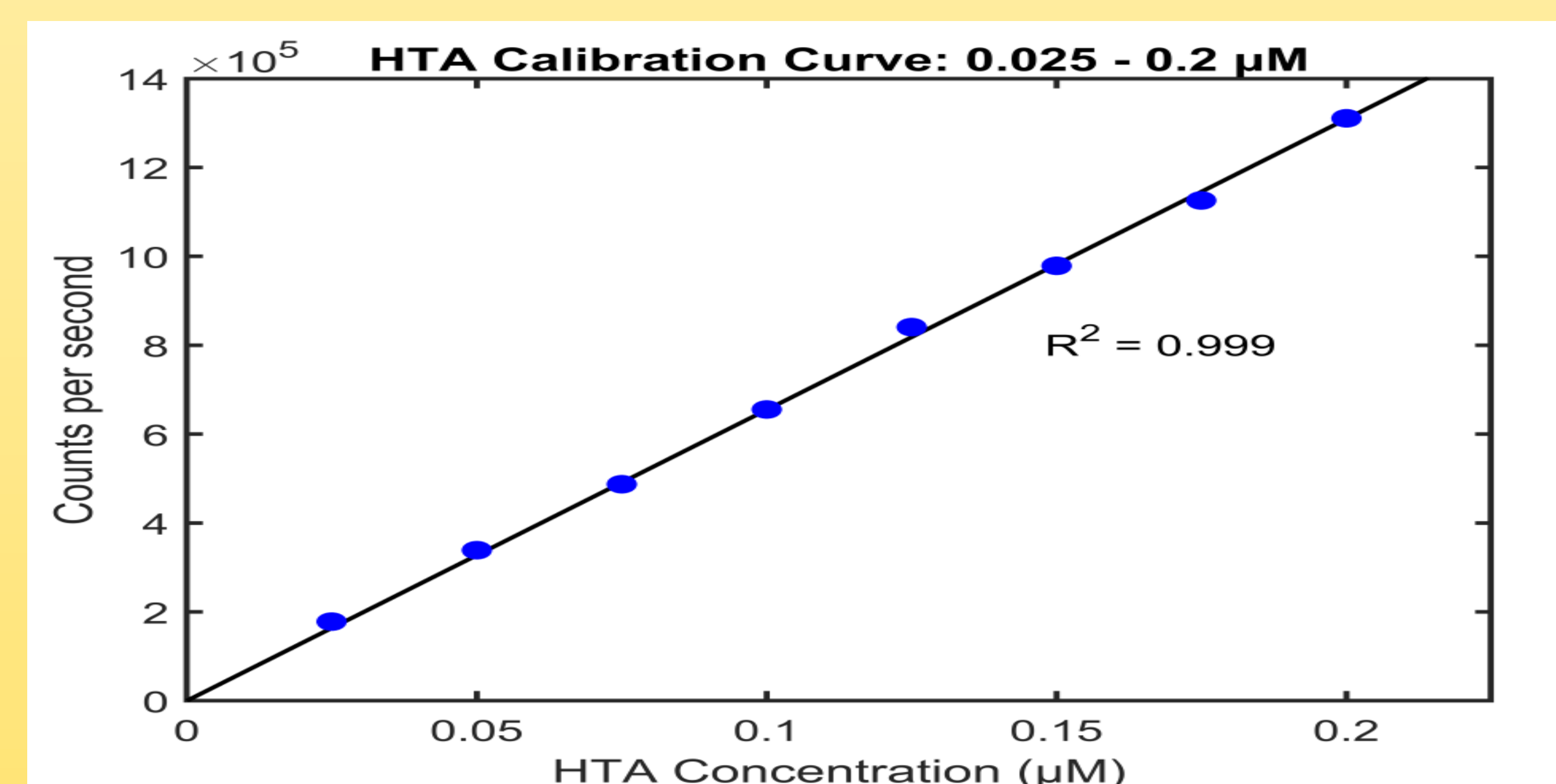


transducer and the nanoparticle-bearing transfer tube were affixed to 3-axis linear translation stages for precise positioning within an ~30 L tank of degassed (20% dissolved O<sub>2</sub>), 10- $\mu$ m filtered water. A stepper-motor enabled vertical translation of the transfer tube through the cavitation field in 0.5 mm increments. Conventional scanline B-mode images were acquired prior to each set of pulses. During specimen sonication, plane wave B-mode and passive images (below) were acquired every 10th trigger pulse to quantify bubble production/location.

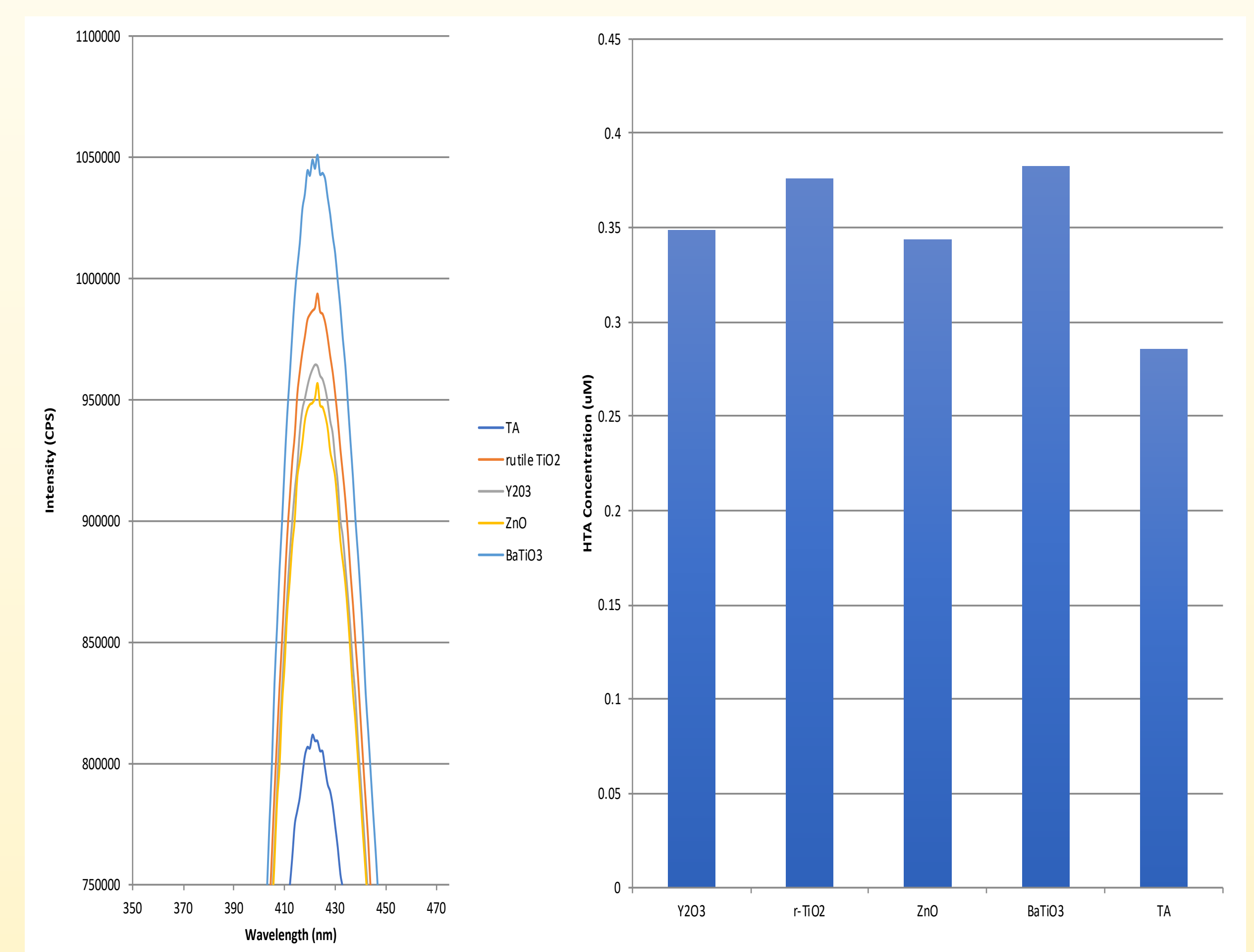


## Results and Discussion

Formation of hydroxyl radicals was quantified by spectroscopic analyses of the shift in relative fluorescence of sonicated samples relative to their corresponding non-sonicated references and controls, as the hydroxyl radicals formed irreversibly converted the



nanoparticle suspension's terephthalic acid (TA) to hydroxyterephthalic acid (HTA). Calibration curves derived from peak fluorescence intensity measurements at 424 nm (ex: 318 nm) revealed the terephthalate assay to be linear over HTA concentrations ([HTA]) spanning 0.025 to 20  $\mu$ M. Pulse duration (PD) and repetition frequency (PRF) had significant impacts on hydroxyl production: increasing PRF from 20 to 100 Hz for 5-cycle pulses raised [HTA] by 1.6x and 2.2x for non-particle and particle specimens, respectively, while increasing PD from 5 to 20 cycles at a PRF of 20 Hz raised [HTA] 3.6x and 5.0x for non-particle and particle specimens, respectively. [HTA] derived from corrected



fluorescence emission spectra of particle bearing specimens revealed up to 34% (BaTiO<sub>3</sub>) enhancement in hydroxyl production compared to comparably sonicated particle-free TA specimens. Surprisingly, however, semiconducting specimens varied less than 11% in hydroxyl production from one another, despite their possessing significantly different dielectric and piezoelectric properties; and comparable in hydroxyl production to wide-gap insulator Y<sub>2</sub>O<sub>3</sub> specimens.

## Conclusions

Although the nanoparticles evaluated in these limited HIFU/histotripsy studies enhanced the production of hydroxyls by ~30%, such production did not appear to be correlated with the nanoparticle's intrinsic dielectric or piezoelectric properties – suggesting, instead, that the nanoparticle's presence simply afforded additional nucleation sites for cavitation-generated ROS rather than ROS arising from sonoluminescence induced photo/sono-excitation of electron/hole pairs on the nanoparticle's surface. Ongoing studies are aimed quantifying the production of other forms of ROS (e.g., H<sub>2</sub>O<sub>2</sub>, <sup>1</sup>O<sub>2</sub>, O<sub>2</sub><sup>-</sup>) under these conditions, as well as correlation of ROS production with sonoluminescence.